Recent Updates for the Heat Transfer Solver in LS-DYNA® with focus on computational welding mechanics

Thomas Klöppel
DYNAmore GmbH, Stuttgart, Germany

Mikael Schill
DYNAmore Nordic AB, Linköping, Sweden

Tobias Loose
Ingenieurbüro Tobias Loose, Wössingen, Germany

Abstract

Even though welding is a well-established production process in manufacturing industries and it has a significant influence on the finished geometry as well as on the material properties of the processed part, it is still often neglected in the virtual process chain. In this contribution novel developments for the heat transfer solver in LS-DYNA® are presented, which are designed to close this gap in the virtual process chain.

First of all, the new keyword *BOUNDARY_THERMAL_WELD_TRAJECTORY is presented that provides an easy and flexible input structure for a heat source moving along a prescribed and, possibly, geometrically complex path for thermo-mechanically coupled and thermal only simulations. As the user can choose from a list of pre-defined equivalent heat source models and this list is very easily extendable, the new feature is potentially applicable to all fusion welding processes.

Due to high temperatures, high temperature gradients and very high temperature rates present in welding applications, phase transformations in the microstructure of the material play a crucial role in the process. The new LS-DYNA material model *MAT_GENERALIZED_PHASE_CHANGE/#MAT_254 allows to distinguish between up to 24 different phases in the microstructure. For each of the possible phase transitions the user can choose from a list of generic and well-established transformation models. Therefore, the model is for example applicable to a wide range of steel and aluminium alloys. Transformation induced plasticity and strains as well as annealing effects have also been incorporated into the new material formulation.

Introduction

Over the last decades the mechanical and functional requirements put on the parts produced by the manufacturing industry has increased tremendously. In order to meet these requirements, the complexity of manufacturing processes has increased likewise. Therefore, numerical process simulation, which aims to accurately predict the shape and properties of the finished part, has gained importance. If the complete process chain is taken into account, simulation enables the optimization of the process already in early design phases.

Many of the processes used today incorporate characteristics of different physical regimes. Naturally, the coupling between different physical fields makes a numerical handling more complex and a powerful multi-physics solver such as LS-DYNA® is indispensable to simulate and solve such complex non-linear coupled problems.

From a numerical point of view, a particularly challenging process step is fusion welding. It is a well-established technology, in which the material is locally heated above the melting point and the molten regions are joined together during subsequent cooling. It usually results in comparably high deformations that have to be compensated for. Within the heat affected zone the material properties are often significantly altered as compared to the base material. This effect is due to phase transformation in the microstructure. Consequently, the main objective of the numerical simulation is to predict the deflection of and microstructure composition in the welded structure.

It is common practice to model the heat input of the weld torch by an equivalent heat source that is described by a power density distribution. For arc welding processes, the Goldak double ellipsoid heat source is considered to be the standard, see Goldak et al. [1]. In LS-DYNA an implementation of this distribution has been available for a couple of years and it can be activated by defining the keyword *BOUNDARY_THERMAL_WELD. In thermo-mechanical coupled simulations the movement and the aiming direction of the weld torch has been associated with the movement of a beam. For curved and possibly deforming structures, an a-priori definition of the movement might be very complex or even impossible.

To address these issues and additionally to provide more flexibility for the shape of the energy rate distribution a new implementation for equivalent heat sources has been added to LS-DYNA. The keyword *BOUNDARY_THERMAL_WELD_TRAJECTORY can be used to simulate a weld torch moving along a path defined on a (possibly moving and deforming) part in coupled but also in thermal-only analyses. In the next section some key feature such as easy definition of trajectories and weld aiming directions, a list of pre-defined weld pool geometries and the possibility of thermal dumping will be discussed.

If the user is mainly interested in the deflection of the part after the welding stage and if the resulting microstructure is thought to play only a secondary role, the LS-DYNA material *MAT_CWM/#270 is a suitable choice to model the welded parts as well as filler material that is commonly used in welding processes, as has been demonstrated in [2]. Nevertheless, many applications necessitate a thorough knowledge of the phase transformations in the heat affected zone and hence of the resulting material properties. LS-DYNA materials *MAT_UHS_STEEL/#244 and *MAT_PHS_BMW/#248 implement phase transformation models tailored for ultra-high strength steel alloys in a press hardening process. Some details on material model *MAT_CWM and also on the main adaptations in *MAT_UHS_STEEL for welding simulations are presented in the third section of this paper. The parameters of the latter are determined based on the chemical composition of the material, which on the one hand allows for a simple input. On the other hand, this connection between phase kinetics and chemical composition restricts the application of the material to only a few steel alloys.

Therefore a new material *MAT_GENERALIZED_PHASECHANGE/#254 has been implemented in order to provide a suitable model for a wide range of metals, particularly in terms of phase kinetics. The material distinguishes between up to 24 different microstructural phases and for each possible phase transformation between them the user can define a specific phase transformation model. The implementation provides a list of generic transformation models proposed in the literature. Important process parameters like transformation induced strains and plasticity are also considered.

Based on the current phase concentrations the mechanical and thermo-mechanical parameters are evaluated. The mechanical characteristics are very similar to what can be found in *MAT_UHS_STEEL, i.e. the material features a temperature and strain rate dependent plasticity algorithm. More details on this material can be found in the fourth section of this contribution. Beside a brief introduction of the keyword input, basic equations of the phase transformation models and the most important features are presented.

A New LS-DYNA®-Keyword for Heat Source Modelling

In case of the *BOUNDARY_THERMAL_WELD implementation the movement of a heat source has always been identified with the movement of two nodal points in the simulation. This firstly implies that a moving heat source can only be modelled in a thermo-mechanically coupled simulation. Secondly, defining the movement and orientation of the heat source on curved parts has often required a significant pre-processing effort. Due to the extremely high temperatures and temperature gradients during welding, the processed part will undergo significant deformations. As this naturally affects the welding path, an a-priori prediction of the path is only seldom possible.

These drawbacks motivated the development of a novel keyword for moving heat sources called *BOUNDARY_THERMAL_WELD_TRAJECTORY. The keyword input reads:

```
*BOUNDARY_THERMAL_WELD_TRAJECTORY
$      PID      PTYP     NSID1      VEL1      SID2      VEL2      NCYC
$    IFORM      LCID         Q     LCROT     LCMOV     LCLAT      DISC
$       P1        P2        P3        P4        P5        P6        P7        P8
$       TX        TY        TZ
```

The implementation of this boundary condition is based on the observation that in most line welding processes the weld torch moves with a prescribed velocity on a pre-defined path. In the numerical representation this trajectory of the root of the weld torch is defined by a node set with the id NSID1, cf. example in Figure 1 on the left. The torch velocity is given by VEL1 and can also be input as load curve defining the velocity as function of time. If the nodes are part of the welded structure, the position of the weld path will be updated automatically with deformation of the structure in a coupled simulation.

Besides the position of the root also the orientation of the heat source is to be defined. The new keyword features three different methods to describe it in order to make the input for many different applications as convenient for the user as possible. The parameter SID2 defines the method to be used by the solver. If it is set to 0, a constant beam aiming direction (tx,ty,tz) is assumed. The corresponding vector is defined in the fourth, optional keyword card. This method has for example been used for the simulations shown in Figure 2.

For curved welds as shown in Figure 3, a constant orientation is probably unrealistic. One possibility to simulate a more reasonable, varying orientation follows ideas used in *BOUNDARY_THERMAL_WELD. For positive values of SID2, it refers to the id of a node set defining a second path. The weld torch is always orientated from points in this path to the root of the torch. The position within the second path is automatically updated using a prescribed velocity (VEL2).
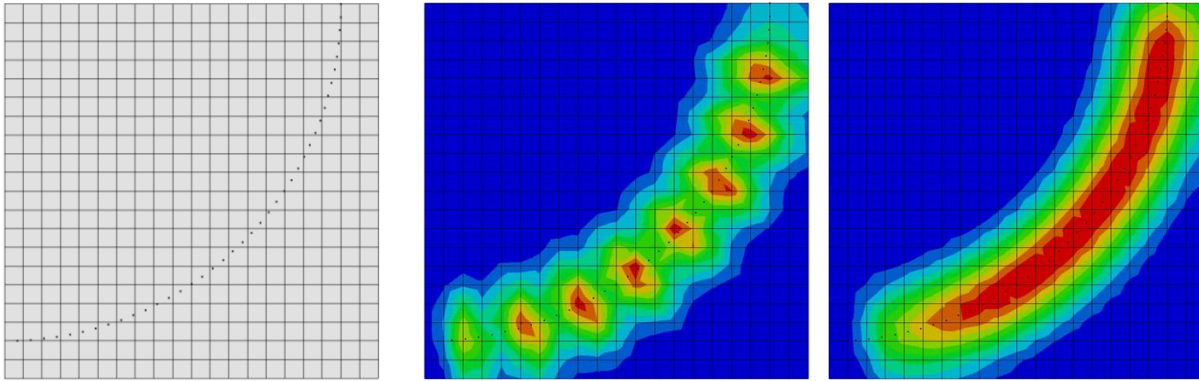
Figure 1: Welding on a trajectory defined on a solid surface: Nodal trajectory (left), temperature fields for a large time step without (middle) and with thermal dumping (right)
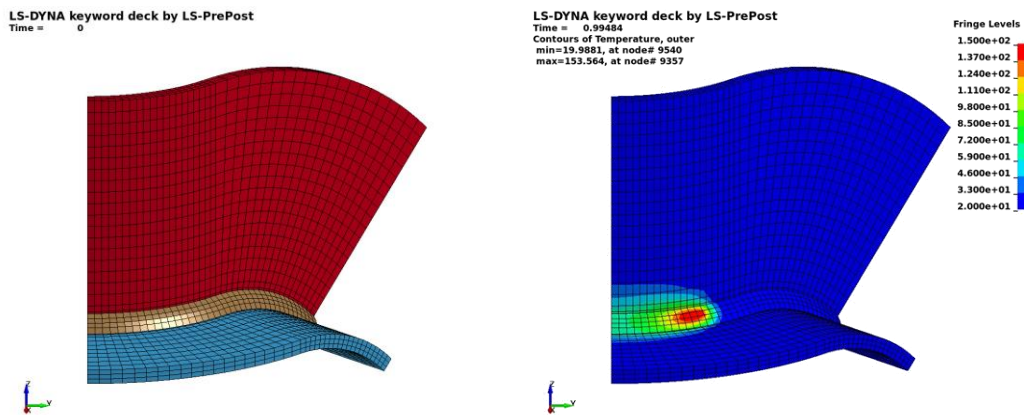

Figure 2: Welding of a curved T-joint. Geometry (left) and temperature field (right)

The usage of a second node set to define the orientation of the weld torch at any given position of the trajectory provides the outmost flexibility for complex welding processes. The disadvantage of this method lies in the significant pre-processing effort, especially for complex weld geometries and sharp curvatures. A remedy could be the third orientation definition that has been implemented into the new boundary condition. It only requires knowledge of the position of the torch and the geometry of the welded structure and is invoked for a negative value of the parameter SID2. The input requires a segment set with an id of –NSID2 and the weld beam is always assumed to be orthogonal to the segments in this set. Many applications in fusion welding show parallels to the curved T-joint in Figure 3. For such applications the third method seems to be the most suitable choice in terms of pre-processing effort and accuracy.

To gain more flexibility and to make variation of process parameters easier, position and orientation can be adapted by time-dependent load curves. The values given in curves LCROT, LCMOV and LCLAT define a rotation around the trajectory, a displacement in weld beam direction and a displacement in lateral direction, respectively. Displacements are applied in the rotated coordinates system.

It is very important to note that due to definitions and functionalities described above, the motion of the weld torch is not necessarily linked to the motion of a structural part as it has been the case for *BOUNDARY_THERMAL_WELD. Consequently, the novel keyword does not require the

presence of a structure solver for modelling a moving heat source but can thus be employed in thermal-only analyses.

The motion of the heat source frequently becomes the limiting factor for the admissible time step size depending on mesh size and torch velocity. Too large time steps result in an unevenly heating with often unphysically high maximum temperatures as can be seen in Figure 2 in the middle. This is due to the fact that by default the solver does not compute intermediate positions and the heat source "jumps" across whole elements. Because the motion of the welding heat source has been transferred from the structure to the thermal solver and is defined by a trajectory, its position can be easily determined at any given point in time. Therefore, a kind of sub-cycling becomes possible, doing NCYC sub time steps for any time step of the thermal solver and smoothing the temperature distribution and equally important the mesh distortion along the trajectory considerably. Moreover, a thermal dumping can be realized to reduce simulation times, cf. Figure 2 on the right.

Although being widely used in industries, the Goldak equivalent heat source might not be the best choice for all applications. The parameter IFORM enables the user to choose between four different equivalent heat source geometries, the parameter of which are P1 to P8. If IFORM is set to 1, the Goldak heat source is defined, with a Gaussian power density distribution on a double ellipsoidal region given as

$$q = \frac{2n\sqrt{n}FQ}{\pi\sqrt{\pi}abc} \exp\left(\frac{-nx^2}{a^2}\right) \exp\left(\frac{-ny^2}{b^2}\right) \exp\left(\frac{-nz^2}{c^2}\right), \tag{1}$$

where a, b, c define the form of the ellipsoid, see Figure 4 on the left. The parameter Q denotes the total power of the heat source. The scaling factor F distinguishes between the forward and the rear part of the heat source. Finally, n is the exponent for the Gaussian distribution.

For an IFORM value of 2 the same double-ellipsoidal region as for the standard Goldak heat source is considered. In contrast a constant power density distribution is assumed instead of (1). In particular for laser welding simulations often double conical or conical heat sources with constant power density distributions are thought to be most suitable. In the keyword they are referred to with IFORM 3 and 4, respectively. The different shapes are sketched in Figure 3.
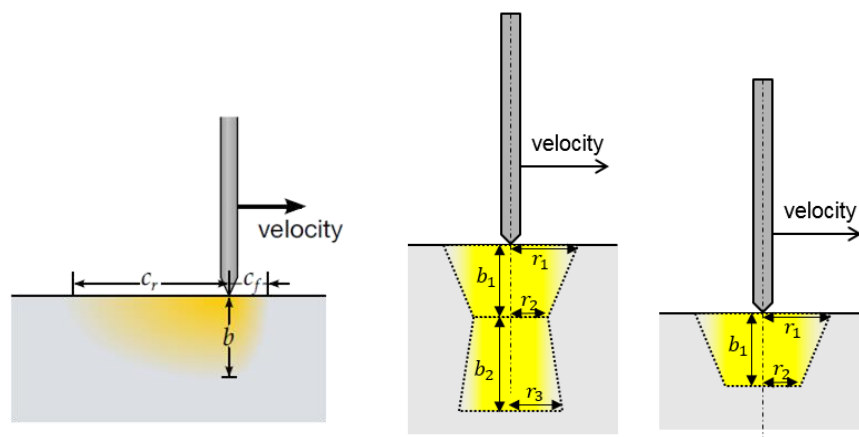

Figure 3: Sketch of different power density distributions: Ellipsoid heat source (left), double conical heat source (middle), conical heat source (right)

The respective power densities have to be integrated on the element level to determine the energy input rate into the structure. The overall power of the weld torch is given by the parameter Q. If the input is a positive number, standard Gaussian quadrature is employed. The computation is fast, but due to geometrical non-linearities in the heat input the obtained accuracy is often not satisfactory. A negative parameter Q invokes a more accurate integration that is based on a subdivision of the elements into cubes with edge length DISCR. Per default a value of 5% of the weld depth is used, but can in most cases be significantly increased to speed-up the simulation without loss of accuracy.

As already mentioned in the introduction welding is in most cases only one of many links in the process chain. Today it is state of the art to use solid discretizations for welding simulations, whereas most of the other process steps are simulated using shell meshes. The new keyword extends the welding functionality in LS-DYNA to shells to enable an easy transition of data between different process stages. Best accuracy can be obtained by using the thermal thick shell formulation, which enables a temperature gradient across the shell thickness of the elements, while any shell formulation implemented in LS-DYNA can be used to solve the mechanical problem.
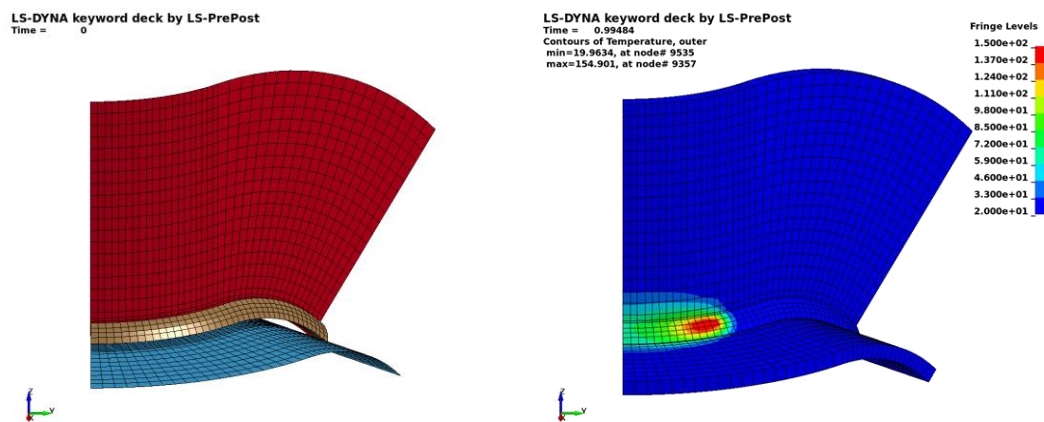

Figure 4: Welding of a curved T-joint discretized with shell elements. Geometry (left) and temperature field (right). Only to visualize the temperature gradients in shell normal direction, the shells are shown as volume elements in post-processing.

The Figures 3 and 5 show equivalent solid and shell meshes for a curved T-joint. In both cases the welded parts and the weld seam are connected with a tied contact formulation and the geometry of the weld pool was chosen such that it exceeds the solid discretization of the weld seam. The resulting temperature fields show an excellent agreement. If the heat input into the shell elements is neglected, the maximum temperature drops by almost 20%. This demonstrates that the new implementation has been necessary to simulate weld processes using shell elements.

Material Models for Welding Simulations

In LS-DYNA, the user can choose from a long list of thermo-mechanical material models. As welding simulations features certain singular characteristics, a few of them have been devised or at least adapted especially for computational welding mechanics (CWM). The most basic and

numerically most efficient of these materials is *MAT_CWM/#270. It is a thermo-elasto-plastic material model based on the von-Mises yield function with isotropic, kinematic or mixed hardening. Moreover, a table input for the coefficient of thermal expansion allows the parameter to be defined as function of current and maximum temperature. This serves as a very simplistic model for the phase change in the microstructure.

The first key feature of *MAT_CWM with respect to its use in welding mechanics is the annealing functionality. Above a certain limiting temperature, history variables such as effective plastic strain and back stresses are re-initialized. The material will show an ideal plastic flow behavior but does not accumulate internal plasticity data.

Welding materials should be applicable not only to the welded structures but also to the weld seams. In those, the material has two different states: until its activation by the weld torch it is in a ghost state, thereafter it is in the solid state as the welded structure. In the ghost state, the material is characterized by negligible thermal and mechanical properties. This reflects the fact that in the real process the filler material is added to the weld seam at the same time the weld torch reaches the specific region. Details on this modelling technique can be found in Lindström [3]. For a validation against experimental data the reader is referred to Lindström et al. [4].

Phase kinetics is represented in *MAT_CWM only in a very simplistic manner that suffices to accurately predict the deflection of the processed part. For detailed studies of the material properties in the heat affected zone more complex material models have to be used. In LS-DYNA, material mode *MAT_UHS_STEEL/#244 and *MAT_PHS_BMW/#248 contain elaborate phase kinetics models, c.f. Åkerström et al. [5], [6] and Hippchen et al. [7], [8]. Both materials expect the input of the chemical composition and the thermos-mechanical properties of the individual phases of the microstructure. The mechanical response of the material is then determined using a linear mixture rule in terms of the current phase contents.

The latest implementation of *MAT_UHS_STEEL also contains the tailored welding features discussed above for *MAT_CWM. The new flag CWM activates an additional input card at the end of the material input.

```
*MAT_UHS_STEEL
$...
$WELDING CARD 11
$  TASTART    TAEND   TLSTART     TLEND    EGHOST    PGHOST    AGHOST
```

Due to numerical reasons the re-set of the history variables for the plasticity algorithm is a continuous process in the temperature range from TASTART to TAEND. The material is assumed to be initially in a ghost state until the temperatures are high enough for activation, which takes place in a range from TLSTART to TLEND. The thermo-mechanical properties of the ghost material are defined by EGHOST (Young's modulus), PGHOST (Poisson's ratio) and AGHOST (coefficient of thermal expansion). More details on the welding capabilities of MAT_UHS_STEEL can be found in [9].

The effect of the ghosting functionality in MAT_UHS_STEEL on the final deformation of a welded T-joint has been studied and is demonstrated in Figure 5. Geometry and heat source definition coincide in both simulation presented, but the material definition used for the weld seam differs. On the left, the material is active right from the start of the simulation, whereas on the

right the weld seam is initially a ghost material activated during simulation by the weld torch. The displacement field significantly differs. The ghosting functionality provides a much weaker joint for the yet de-activated areas and thus provides a more realistic result.
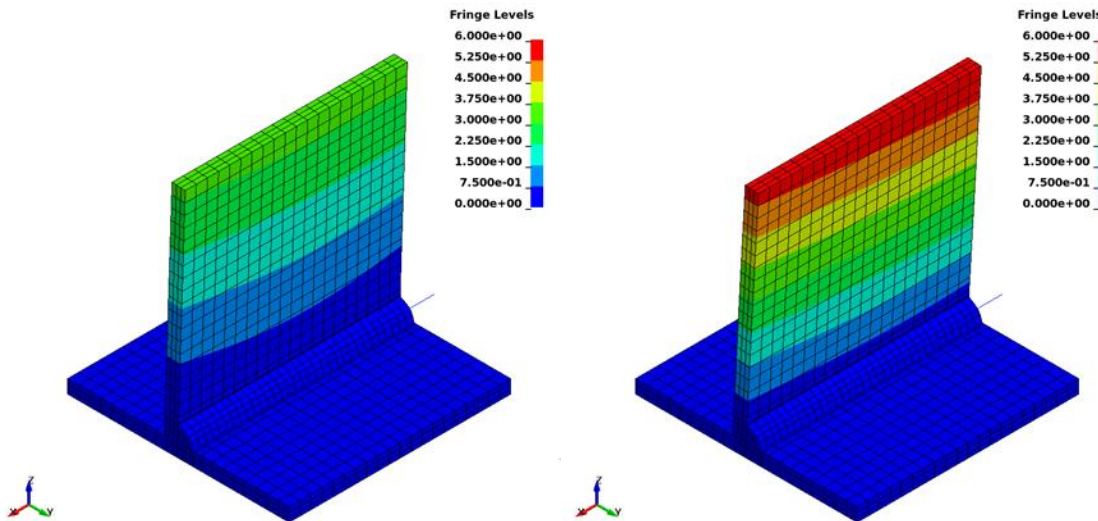

Figure 5: Welding of a T-joint. On the left, all material is activated at the beginning, on the right, ghost material is used as filler material. Color coded is the displacement magnitude.

As mentioned above, the parameter set for the phase transformation formulation in *MAT_UHS_STEEL and also in *MAT_PHS_BMW are based on the chemical composition. The main advantage of this approach is a relatively easy input. Unfortunately, the heuristic formulas that are internally used to map the chemical to thermo-mechanical parameters are only valid for 22MnB5 steel grades usually used in press hardening processes and the material formulation only poorly describes other frequently used steel grades or even different materials such as aluminum. To be applicable to a wider range of metals, a direct input of the transformation parameters as well as the thermo-mechanical parameters seems indispensable. The novel material formulation *MAT_GENERALIZED_PHASECHANGE/#254 aims to implement a generic approach for modelling phase transformations. Some details on the current status of the material is given in the next section.

The Novel Material *MAT_GENERALIZED_PHASECHANGE

Following the discussion above the main objective of the new implementation is to provide a suitable material formulation for a large range of metals used in welding and heat treatment applications. Therefore, the LS-DYNA material *MAT_GENERALIZED_PHASECHANGE/#254 accounts for up to 24 phases and it is important to note that the phases are not hard-coded to represent a certain microstructure phase as it has been the case for the five phases in *MAT_UHS_STEEL. The user has to decide which of the possible phase transformations is to be considered and what transformation law from a list of well-established transformation laws is most suitable for the respective transformation. Each of the models requires a different set of parameters. Naturally such a generic approach provides great flexibility, but goes along with a more complex material parameterization.

At present, the implementation is only available for solid elements. The keyword of the material consists of up to eight cards:

```
*MAT_GENERALIZED_PHASECHANGE
$     MID       RO        N       YM       PR      MIX     MIXR
$  TASTART    TAEND   TABCTE                                      DTEMP     TIME
$    PTLAW    PTSTR    PTEND     PTX1     PTX2     PTX3     PTX4     PTX5
$   PTTAB1   PTTAB2   PTTAB3   PTTAB4   PTTAB5
$    PTEPS     TRIP                               GRAI
$    LCY01    LCY02    LCY03    LCY04    LCY05    LCY06    LCY07    LCY08
$    LCY09    LCY10    LCY11    LCY12    LCY13    LCY14    LCY15    LCY16
$    LCY17    LCY18    LCY19    LCY20    LCY21    LCY22    LCY23    LCY24
```

The thermo-mechanical formulation itself is similar to what can be found in other LS-DYNA materials and particularly in*MAT_UHS_STEEL: the material features a von-Mises plasticity depending on temperature, strain rate and phase concentrations. Parameters YM, PR and TABCTE for Young's modulus, Poisson's ratio, and coefficient of thermal expansion, respectively, can be given as functions of phase and temperature. The temperature and strain rate dependent yield curves for the individual phases are defined using the parameters LCYi. The number of phases to be considered is given by N and the initial concentrations by the load curve MIX. From the micro-structure composition, the thermo-mechanical properties are calculated using a possibly temperature dependent linear mixture rule defined by MIXR.

As discussed above, reset of history data for the plasticity algorithm is an important effect the material has to capture to be applicable to welding simulations. In the new formulation, the corresponding temperature range can again be defined with parameters TASTART and TAEND. The material formulation does not necessitate a distinguished ghost state since inactive material can just be identified with one of the microstructure phases and is transformed into an active phase during heating.

For the calculations of the micro-structure evolution a new concept has been implemented. Phase changes are controlled by the two-dimensional transformation matrix PTLAW, where the first dimension is the base phase and the second the generated phase. This implies that for any phase to be transformed a load curve is specified in the *DEFINE_TABLE(_2D). The load curve defines the phase transformation law as function of the resulting phase. For any of the defined transformations starting and end temperature have to be defined. These parameters are expected to be given in the same matrix form and defined by tabular data in PTSTR and PTEND.

In the current state of the implementation four different micro-structure models are accounted for. If the phase transformation laws 1 (cooling) or -1 (heating) are chosen in the respective load curve, the so-called Koistinen-Marburger model, see [10], is used. It is widely accepted for diffusionless processes. It calculates the generated phase concentration x_b as function of the current temperature T and the transformed phase x_a using the formula

$$x_b = x_a\left(1.0 - e^{-\alpha\,\kappa\,(T_{start}-T)}\right). \tag{2}$$

In this equation the parameter κ is 1.0 for cooling and -1.0 for heating. Equation (2) requires only the scalar-valued Koistinen-Marburger factor α. It is defined in the appropriate spot in the table referred to by PTX1.

The second transformation model implements one of the most widely used laws for diffusive phase transformations: the extended Johnson-Mehl-Avrami-Kolmogorov (JMAK), see for example review in [11]. Based on an temperature depending equilibrium concentration $x_{eq}(T)$ and a relaxation time $\tau(T)$ the differential form

$$\frac{dx_b}{dt} = n(T)(k_{ab}x_a - k'_{ab}x_b)\left(\ln\left(\frac{k_{ab}(x_a + x_b)}{k_{ab}x_a - k'_{ab}x_b}\right)\right)^{\frac{n(T)-1.0}{n(T)}} \tag{3}$$

with parameters $k_{ab} = \frac{x_{eq}(T)}{\tau(T)}f(\dot{T}), k'_{ab} = \frac{1.0-x_{eq}(T)}{\tau(T)}f'(\dot{T})$

defines the transformation from x_a to x_b. The functions $f(\dot{T})$ and $f'(\dot{T})$ are correction functions accounting for temperature rate effects. For a constant exponent $n(T) = 1$ equation (3) reduces to the so-called Leblond model [12]. The model is applicable for heating (law -2) and cooling (law 2). It requires the input of the temperature and temperature rate dependent parameters $n, x_{eq}, \tau, f, \dot{f}$, which are defined in this order by three-dimensional tables PTTAB1 to PTTAB5.

For cooling the model proposed by Kirkaldy and Venugopalan [13] can also be employed. It has been added to the list of transformation laws (choose 3 to use) since it is the base of microstructure evolution in MAT_UHS_STEEL. In a general form the formulation can be written as

$$\frac{dX_b}{dt} = 2^{0.5(G-1)}f(C)(T_{start} - T)^{n_T}D(T)\frac{X_b^{n_1(1.0-X_b)}(1.0 - X_b)^{n_2 X_b}}{Y(X_b)}. \tag{4}$$

It is noteworthy that here a normalized phase concentration X_b is calculated. It has to be transformed into the total phase concentration x_b by $x_b = X_b x_{eq}(T)$, with equilibrium concentration $x_{eq}(T)$. The list of necessary parameters comprise the four scalar-valued parameters $f(C), n_T, n_1, n_2$ defined in PTX1 to PTX4 and three functions $D(T), Y(X_b), x_{eq}(T)$ defined in PTTAB1 to PTTAB3. The grain size G in equation (4) coincides with the parameter GRAIN.

Finally, the phase kinetics in *MAT_UHS_STEEL during heating is governed by the model of Oddy et al. [14]. It has been added to *MAT_GENERALIZED_PHASECHANGE as model -4 and uses the evolution equation

$$\frac{dx_b}{dt} = n \cdot \frac{x_a}{c_1(T - T_{start})^{-c_2}} \cdot \left(\ln\left(\frac{(x_a + x_b)}{x_a}\right)\right)^{\frac{n-1.0}{n}}. \tag{5}$$

For usage only three scalar parameters are required: n, c_1, c_2. As before these parameters are taken from data in the two-dimensional tables PTX1 to PTX3.

For most steel alloys, phase transition between ferritic and austenitic phases goes along with transformation induced strains. In dilatometer experiments these show as characteristic jumps in strain over temperature curves. The height of the jumps varies with temperature and naturally with the phase combinations. This information about the jumps can serve as input for the new material formulation as tabular data in parameter PTEPS. As Figure 6 (left) demonstrates the new material can capture these jumps between different dilatometer curves for the individual phases.
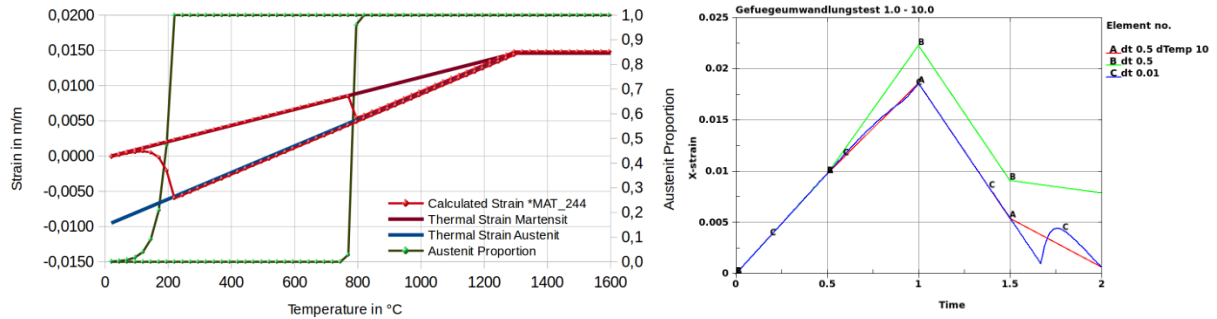
Figure 6: The effect of transformation induced strains: Dilatometer experiment on the left, the effect of different time step sizes and the parameter DTEMP on the right.

Different coefficients of thermal expansion for the phases and transformation induced strains add significant non-linearities with respect to the temperature to the material. Welding simulations usually feature locally extremely high temperature rates and temperature gradients due to the high power input of the applied weld sources. Therefore, using a reasonably large time step with respect to simulation time will lead to a temperature increase of several hundred Kelvin at some nodes within one time step. The strain results for one rapidly heated element are shown in Figure 6 on the right. The obtained curves for a large time step (B) and a very small time step (C) deviate significantly. Therefore, a parameter DTEMP has been added, that represents the temperature increase within one time step that still shows acceptable results. In case that during the material evaluation at an integration point a higher temperature rise is detected, a sub-cycling procedure is invoked assuming a constant temperature rate. The quality of the strain results can be significantly improved by this approach as curve (A) shows. As the sub-cycling is only done at certain regions, the simulation time is only mildly affected for realistic examples.

Phase transformations do not only induce elastic but also plastic strains. The algorithm to calculate the transformation induced plasticity (TRIP) is based on the formulation proposed by Leblond [15]. This formulation has a very high impact on the residual stress distribution of welded structures and can be activated by defining a non-zero value for the parameter TRIP.

In Figure 7 the simulation of the Nitschke-Pagel [16] experiment is depicted. In this bead on plate example, a weld torch is moved along the middle of a steel block. Filler material is not present. In this case experimental and numerical data for the residual stresses in the structure is available in [17] and can be compared with simulation results of LS-DYNA using the new formulation *MAT_GENERALIZED_PHASECHANGE.

The residual stresses are shown in Figure 8. Along a line on the surface of the structure, see Figure 8 (left), stress data can be used for quantitative comparison with measurements from [16]. The numerical approximation obtained with *MAT_GENERALIZED_PHASECHANGE for both the longitudinal and the transversal component agree reasonably well with the literature data. The same investigation has been made for a specialized welding simulation code in [17]. Although the material definitions and also the formulation for the equivalent heat source slightly differ between the two numerical models, there is a good agreement between the numerical results.
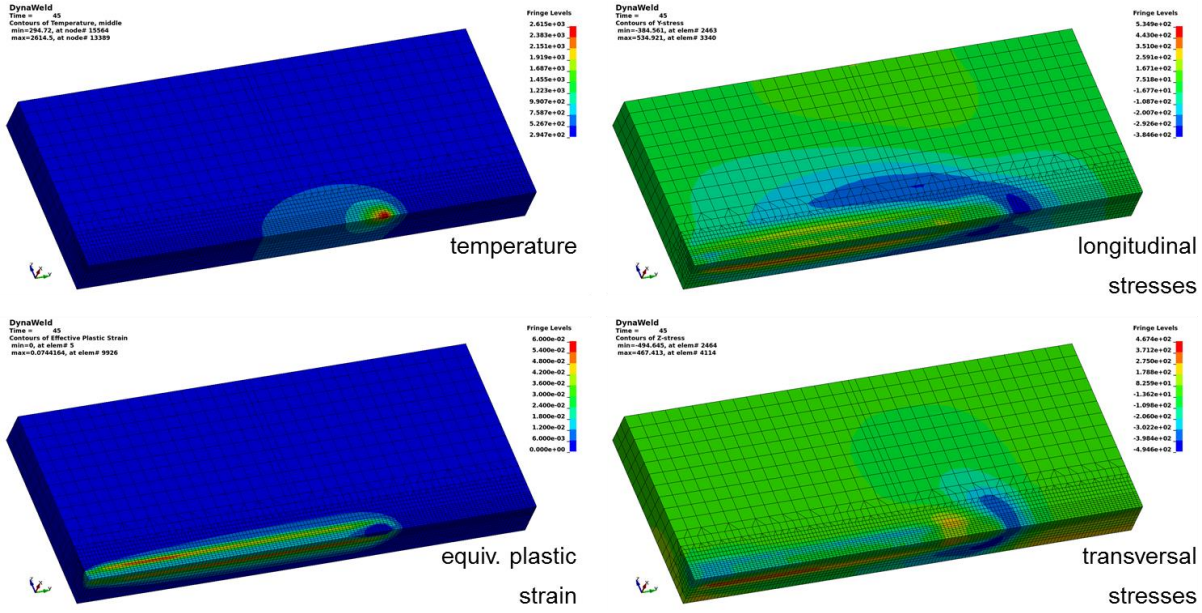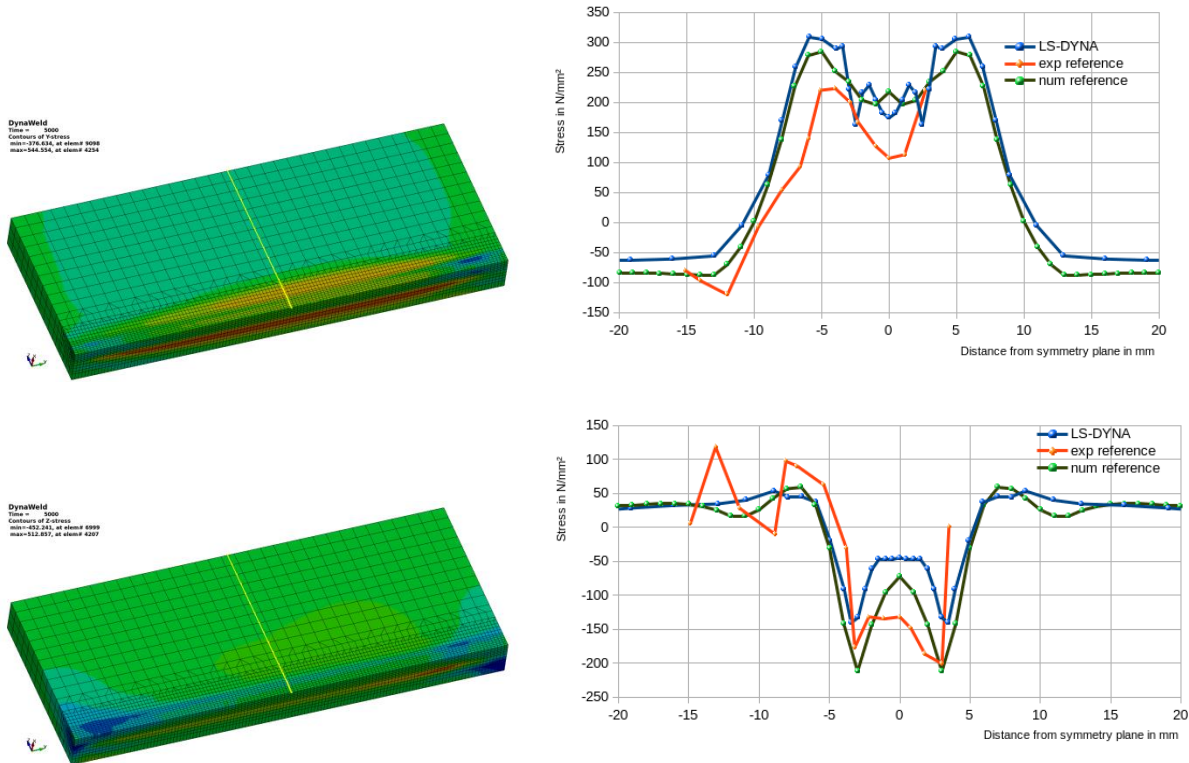
Figure 7: Simulation of the Nitschke-Pagel test at time t=45s

Figure 8: Residual stresses for Nitschke Pagel test after cooling.

Outlook

As welding is very important for manufacturing industries some effort has been put into novel features of the multi-physics Finite Element solver LS-DYNA for more accurate numerical simulations and easier set-up of this very complex coupled process. The development shown in this contribution will continue in order to further improve the welding capabilities of the software and still widen its field of application.

The new thermal boundary condition *BOUNDARY_THERMAL_WELD_TRAJECTORY will be extended by further pre-defined energy rate distribution functions but also by the possibility to input user-defined function in the local weld coordinate system.

The next step in the development of the *MAT_GENERALIZED_PHASECHANGE is the implementation for shell elements. So far material formulation has only been used to model steel alloys, but most of the equations discussed above also apply aluminum alloys. Adaptations to the model will be made to account for both groups of metals.

References

[1]　J. Goldak, A. Chakravarti and M. Bibby, "A Double Ellipsoid Finite Element Model for Welding Heat Sources," *IIW Doc.No.212-603-85,* 1985.

[2]　M. Schill and E.-L. Oldenberger, "Simulation of residual deformation from a forming and welding process using LS-DYNA," in *Proc. of 13th International LS-DYNA Conference*, Detroit, 2014.

[3]　P. Lindström, "DNV Platform of Computational Welding Mechanics," in *Proc. Of Int. Inst. Welding 66th Annual Assembly* , 2013.

[4]　P. Lindström, L. Josefson, M. Schill and T. Borrvall, "Constitutive Modelling and Finite Element Simulation of Multi Pass Girth Welds," in *Proc. Of NAFEMS NORDIC Conference*, Gothenburg, 2012.

[5]　P. Åkerström and M. Oldenburg, "Austenite decomposition during press hardening of a boron steel – Com-puter simulation and test," *Journal of Materials Processing Technology,* vol. 174, pp. 399-406, 2006.

[6]　P. Åkerström, G. Bergman and M. Oldenburg, "Numerical implementation of a constitutive model for simu-lation of hot forming," *Modeling and Simulation in Materials and Engineering,* vol. 15, pp. 105-119, 2007.

[7]　P. Hippchen, M. Merklein, A. Lipp, M. Fleischer, H. Grass and P. Craighero, "Modelling kinetics of phase transformation for the indirect hot stamping process," *Key Engineering Materials,* vol. 549, pp. 108-116, 2013.

[8]　P. Hippchen, A. Lipp, H. Grass, P. Craighero, M. Fleischer and M. Merklein, "Modelling kinetics of phase transformation for the indirect hot stamping process to focus on car body parts with tailored properties," *Journal of Materials Processing Technology,* vol. 228, pp. 59-67, 2016.

[9]　T. Klöppel and T. Loose, "Recent developments for thermo-mechanically coupled simulations in LS-DYNA with focus on welding processes," in *Proc. of 10th European LS-DYNA Conference*, Wuerzburg, 2015.

[10] M. Koistinen and R. Marburger, "A General Equation Prescribing the Extent of the Austenite-Martensite-Transformation in Pure Iron Carbon-Alloys and Plan Carbon Steels," *Acta Metallurgica,* vol. 7, pp. 59-60, 1959.

[11] M. Fanfoni and M. Tomellini, "The Johnson-Mehl-Avrami-Kolmogorov model: A brief review," *Il Nuovoto Cimento D,* vol. 20, pp. 1171-1182, 1998.

[12] J. Leblond and J. Devaux, "A New Kinetic Model for Anisothermal Metallurgical Transfromations in Steels Including Effect of Austenits Grain Size," *Acta Metallurgica,* vol. 32, pp. 137-146, 1984.

[13] J. Kirkaldy and D. Venugopalan, "Prediction of microstructure and hardenability in low alloy steels," in *Internalional conference on phase transformation in ferrous alloys*, Philadelphia, 1983.

[14] A. Oddy, J. McDill and L. Karlsson, "Microstructural predictions including arbitrary thermal histories, reaustinitization and carbon segregation effects," *Canadian Metallurgical Quarterly,* vol. 35(3), pp. 275-283, 1996.

[15] J. Leblond, "Mathematical modelling of transformation plasticity in steels ii: Coupling with strain hardening phenomena," *International Journal of Plasticity,* vol. 5, pp. 573-589, 1989.

[16] T. Nitschke, "Untersuchungen zum Einfluß des Vorwärmens auf den Eigenspannungszustand von WIG-geschweißten Platten aus St 52-3 und StE70," Institut für Werkstofftechnik der Universität-Gesamthochschule Kassel, 1985.

[17] T. Loose, "Einfluß des transienten Schweißvorganges auf Verzug, Eigenspannungen und Stabiltiätsverhalten axial gedrückter Kreiszylinderschalen aus Stahl," Universität Karlsruhe (TH), 2007.